Journal of Cellular Biochemistry 102:1234–1244 (2007)

Nanomechanotransduction and Interphase Nuclear Organization Influence on Genomic Control

Matthew J. Dalby,[1]* Nikolaj Gadegaard,[2] Pawel Herzyk,[3] Duncan Sutherland,[4] Hossein Agheli,[4] Chris D.W. Wilkinson,[2] and Adam S.G. Curtis[1]

[1]Centre for Cell Engineering, Joseph Black Building, Institute of Biomedical and Life Sciences, University of Glasgow, Glasgow, G12 8QQ, Scotland, UK
[2]Centre for Cell Engineering, Rankine Building, Department of Electronics and Electrical Engineering, University of Glasgow, Glasgow, G12 8QQ, Scotland, UK
[3]Sir Henry Wellcome Functional Genomics Facility, Joseph Black Building, Institute of Biomedical and Life Sciences, University of Glasgow, Glasgow, G12 8QQ, Scotland, UK
[4]iNANO Interdisciplinary Research Center, University of Aarhus, Aarhus 8000, Denmark

Abstract The ability of cells to alter their genomic regulation in response to mechanical conditioning or through changes in morphology and the organization of the interphase nuclei are key questions in cell biology. Here, two nanotopographies have been used as a model surfaces to change cell morphology in order to investigate spatial genomic changes within the nuclei of fibroblasts. Initially, centromeres for chromosome pairs were labeled and the average distance on different substrates calculated. Further to this, Affymetrix whole genome GeneChips® were used to rank genomic changes in response to topography and plot the whereabouts on the chromosomes these changes were occurring. It was seen that as cell spreading was changed, so were the positions along the chromosomes that gene regulations were being observed. We hypothesize that as changes in cell and thus nuclear morphology occur, that this may alter the probability of transcription through opening or closing areas of the chromosomes to transcription factors. J. Cell. Biochem. 102: 1234–1244, 2007. © 2007 Wiley-Liss, Inc.

Key words: mechanotransduction; microarray; nanobiotechnology; Interphase Nuclear Organization

There is increasing evidence that cells can act as mechanosensitive units responding to the mechanical stimulation of the extracellular matrix though focal adhesions and changes in cytoskeletal organization. Mechanotransduction can take two broad forms, indirect and direct. The indirect route involves changes in positioning of ion channels, G-proteins and kinases [Burridge and Chrzanowska-Wodnicka, 1996] through, for example, stretch [Eastwood et al., 1998] or contact guidance [Clark et al., 1991]. This leads to induction/reduction of signaling cascades thus altering cellular behavior, for example, proliferation or differentiation.

The direct form probably involves changes in tension through the cytoskeleton from relaxed morphology (rounded) to strained morphology (spread) and intermediate shapes [Ingber, 1993; Charras and Horton, 2002; Dalby, 2005]. Direct mechanotransduction has clear roles in regulation of blood pressure, vascular response to fluid shear stress, bone remodeling, maintenance of muscle, and perception of touch and sound [Katsumi et al., 2004].

It is known that the extracellular environment can cause extremes of morphology with hydrophobic surfaces generally giving poor cellular adhesion and hence a rounded morphology [Martines et al., 2005] to grooved surfaces (topographical or chemically printed) or uniaxially stretched surfaces leading to cellular extension [Clark et al., 1991; Eastwood et al., 1998]. Chemical and topographical patterning can also be used to confine cells in shapes that

*Correspondence to: Matthew J. Dalby, Centre for Cell Engineering, Joseph Black Building, Institute of Biomedical and Life Sciences, University of Glasgow, Glasgow, G12 8QQ, Scotland, UK. E-mail: m.dalby@bio.gla.ac.uk

Received 5 March 2007; Accepted 6 March 2007
DOI 10.1002/jcb.21354

can define their ability to survive and even differentiate [Whitesides, 2003].

How the cytoskeleton can transduce mechanical signals to the nucleus is a matter for great debate. An interesting theory is that of cellular tensegrity, whereby an integrated cytoskeleton (microfilaments (MFs), microtubules (MTs), and intermediate filaments (IFs)) has the ability to form structures supported by tensile elements [Ingber, 1993, 2003a,b]. It is thought that IFs could also be involved in a tensile role. In order to have tensegrity, the structure must be pre-stressed. In a cell, this would be provided by MFs contracting against focal adhesions (acting as cellular guy wires). Variations on Ingbers original model and other theories, such as percolation, have also been proposed [Forgacs, 1995; Charras and Horton, 2002].

What is clear is that first, the Young's moduli of the individual cytoskeletons would suggest that they would have to transduce mechanical signals via tension as perhaps only bundled MFs could transmit compressive force. Second, that the cytoskeleton would have to work in an integrated manner as direct mechanotransduction relies on the movement of force from the focal adhesions to the nucleus. MFs, and to some extent MTs are linked to adhesions, neither are directly linked to the nucleus. Cytoskeletal IFs, however, are linked to the nuclear lamins (the nucleoskeletal IFs) [Bloom et al., 1996; Foster and Bridger, 2005]. Third, it seems that the inhomoginity the cytoskeleton provides the cytoplasm is essential for long-distance force propagation [Wang and Suo, 2005].

Studies have also provided evidence in muscle cells that IFs can transmit stress signals to chromatin [Bloom et al., 1996] and that in reaction to tension, the IFs reorient leading to nuclear distortion and nucleoli rearrangement along the applied axis [Maniotis et al., 1997b]. This signaling could happen through cytoskeletal IF interaction with nucleoskeletal IFs and be transmitted to DNA via the close relationship of lamins and chromatin, specifically telomeres [Bloom et al., 1996; Molenaar et al., 2003].

Consistent with the above is evidence that the nucleus can expand in response to tension through expansion of the laminar network. The structure of the network is, however, resistant to compressive changes [Dahl et al., 2004]. A further study has also shown that changes in cell morphology due to the topography of the extracellular environment results in changes of lamin morphology [Dalby et al., 2007]. Relaxed cells with a more rounded morphology have a dense lamin network, well spread cells under tension have a more diffuse lamin network.

A key question however, is that assuming that mechanical signals can be transduced to the nucleus, how are these signals translated into genomic changes? We would like to propose a model whereby that due to the linking of the telomeric ends of interphase chromosomes (Chs) to the lamin network, changes in morphology can open or close areas of DNA to transcription.

It is becoming accepted that rather than the Chs being randomly arranged during interphase, that there is a consistency of position [Heslop-Harrison et al., 1993]. In fact, it is considered that Chs occupy discrete territories within the nucleus [Cremer and Cremer, 2001].

A number of early investigators observed filaments (possibly of DNA) connecting interphase Chs, for example, [Hoskins, 1965]. Later, Fey [Fey et al., 1984] showed that in interphase cells, the nuclear matrix appears to interconnect different nuclear components, such as nucleoli, to each other and the surrounding cytoskeleton. More recently, it has been shown that the human endothelial cell genomes behave as a continuous, elastic structure [Maniotis et al., 1997a,b].

These observations allow speculation that there may be mechanical continuity from the extracellular matrix to the cytoskeleton via focal adhesions, to the nucloskeleton and then onwards to the Chs and that changes in gene positioning lead to changes in genome regulation. This report studies this hypothesis using two test surfaces that reduce cellular adhesion to different degrees, one that gives a slight reduction of tension and one that gives a large reduction in tension and then plots positioning (band position) of changes in genome regulation on long (Ch 3) and medium (Ch 11) and short (Ch 16) Chs (bands are numbered from the centromere outwards, and correspond well to similar measurements made in centimorgans or magabases). Affymetrix human genome GeneChips and human fibroblasts were used to allow plotting of the gene changes. Rank product (RP) bioinformatics analysis was used to assess the changes and derive groups of changed genes to plot against unchanged genes. Also chromosome painting of centromere pairs was used to

measure the distance between centromeres to assess if changes in tension confer changes in interphase chromosomal organization.

This current study forms a follow-on from a recent article focusing on linking nuclear and lamin morphology changes to morphological and cytoskeletal changes resulting from nanotopographical environment [Dalby et al., 2007].

MATERIALS AND METHODS

Materials

Electron beam lithography. Silicon substrates were coated with ZEP 520A resist to a thickness of 100 nm. After the samples were baked for a few hours at 180°C they were exposed in a Leica LBPG 5-HR100 beamwriter at 50 kV. We have developed an efficient way to pattern a 1 cm^2 area with 1–10 billion pits [Gadegaard et al., 2003]. An 80 nm spot size was used with a pitch of 300 nm. After exposure the samples were developed in *o*-xylene at 23°C for 60 s and rinsed in copious amounts of iso-2-propanol.

Colloidal lithography. The 1 mm thick Silicon substrates were precut into 2 cm by 2 cm squares using a diamond saw (Load point). A thin film of PMMA with 50 nm thickness on the each silicon substrates prepared by spin coating 2% PMMA (950 k) in anisole solution at 8,000 rpm and baked on a hot plate at 170°C for 2 min.

Colloidal lithography method was used to produce nanostructured features on the substrates. This approach is described in detail elsewhere [Denis et al., 2002; Hanarp et al., 2003], but in brief utilizes electrostatically assembled dispersed monolayers of colloidal particles as masks for pattern transfer into substrate materials. In this work the substrate materials were pretreated with a light oxygen plasma (0.25 Torr, 50 w RF, 5 s Batchtop) followed by electrostatic self-assembly of a multilayer of polyelectrolytes (poly (diallyldimethylammonium chloride) (PDDA, MW 200,000–350,000, Aldrich), poly (sodium 4-styrenesulfonate) (PSS, MW 70,000, Aldrich) and aluminium chloride hydroxide (ACH, Reheis)). Subsequent assembly of a colloidal mask (sulphate modified polystyrene colloid 107 nm ± 5 nm IDC) from aqueous solution followed by drying resulted in a dispersed colloidal monolayer which has short range order, but no long range order.

The pattern of the colloidal mask was transferred into the substrates by collimated Ar ion bombardment (CAIBE Ion Beam System—Oxford Ionfab—500 eV 0.2mA/cm^2, 15 degrees off of normal incident angle for 10 min) resulting polymeric hemispherical structures standing on silicon surface (referred to as Hemi). The samples were checked using atomic force microscopy (AFM).

Nickel electroplating. Nickel dies were made directly from the patterned samples. A thin (50 nm) layer of Ni-V was sputter coated on the samples. This layer acted as an electrode in the subsequent electroplating process. The dies were plated to a thickness of ca. 300 μm.

Cleaning process for nickel shims. Once returned from the plater, the nickel shims were cleaned by firstly stripping the polyurethane coating (used for protection during shipping) using chloroform in an ultrasound bath for 10–15 min. Second, silicon residue was stripped by being wet etched in 25% potassium hydroxide at 80°C for 1 h. Shims were rinsed thoroughly in reverse osmosis H_2O, air gun dried and were checked using AFM. The shims were finally trimmed to approximately 30 × 30 mm sizes using a metal guillotine.

Nanoimprinting procedure. Imprints of the nickel shims into PMMA were achieved using an Obducat nanoimprinter (temperature = 180°C, pressure = 15 Bar, time = 300 s). The imprints were trimmed and then measurements (AFM) made of random samples.

Planar PMMA was used as a control.

Cell Culture

Infinity™ Telomerase Immortalized primary human fibroblasts (hTERT-BJ1, Clonetech Laboratories, Inc.) were seeded onto the test materials at a density of 2×10^4 cells/ml of medium. The medium used was 71% Dulbeccos Modified Eagles Medium (DMEM) (Sigma, UK), 17.5% Medium 199 (Sigma, UK), 9% fetal calf serum (FCS) (Life Technologies, UK), 1.6% 200 mM L-glutamine (Life Technologies, UK) and 0.9% 100 mM sodium pyruvate (Life Technologies, UK). The cells were incubated at 37°C with a 5% CO_2 atmosphere. Cells were seeded onto the test and control materials (4 replicates, 2.5 cm^2 area for each sample) at a density of 1×10^4 cells ml^{-1}.

Image Analysis of Cell Morphology

After four days of culture, the cells on the test materials were fixed in 4% formaldehyde/PBS

at 37°C for 15 min. The cells were then stained for 2 min in 0.5% Coomassie blue in a methanol/acetic acid aqueous solution, and washed with water to remove excess dye. Samples could then be observed by light microscopy and automated detection of cell outline was used to calculate individual cell areas. The image analysis software was downloaded from the National Institute of Health (USA) (Image J, http://rsb.info.nih.gov/ij/). Between 50 and 60 cells were counted, and standardized illumination conditions were used throughout.

Centromere Labeling

After 4 days of culture for three material replicates, cells were fixed for 5 min in 3:1 methanol/glacial acetic acid. After fixation, the cells were dehydrated in 70%, 90%, and 100% ethanol (2 min × 2 for each grade). Next, the cells were placed in 0.1% pepsin for 5 min before washing with 2 × SSC and dehydrating for a second time. After dehydration, the cells were baked at 65°C for 1 h.

Biotin conjugated probes for centromeres of Chs 3, 11, and 16 (CamBio, UK) were warmed to 65°C for 5 min. The probes (pooled to the desired amount, 10 μl per sample) were next denatured at 80°C for 10 min and allowed to preanneal at 37°C for 10 min.

After baking, the cell preparations were denatured in 70% formamide/2 × SSC for 2 min before quenching in ethanol and repeating the dehydration step. The denatured, preannealed probe was then added to the cells, a cover slip placed on top and hybridized at 37°C overnight. Labeling and amplification with FITC was performed the next day according to manufacturers protocol using an amplification kit (CamBio, UK). Nuclei were counterstained with propridium iodide prior to viewing (total of 25 cell observations for each material). Centromere distances calculated in ImageJ.

Imaging

For all fluorescence imaging, a Zeiss Axiovert 200M was used alongside an evolution OEi camera and Image Pro-Plus Software (Media Cybernetics). A Zeiss Plan Neofluor 100× (1.3 NA) lens was used for centromere observation and a 10× (0.15 NA) for morphological image analysis. All microscopy was performed at room temperature using Vectorshield mounting medium (Vector Laboratories, UK).

Statistics

All results were observed to be skewed to the left and were thus $\log_2$ transformed before use of one-way ANOVA (Turkey) using SigmaStat® software.

Microarray

Affymetrix® whole genome human GeneChips® were used according to manufacturer's instructions (included). Briefly, after 21 days of culture, RNA was extracted from the cells from four replicates of each material using a Stratagene (Amsterdam, Netherlands) RNA miniprep kit. The RNA was amplified using a GeneChip® Small Sample Target Labeling Assay Kit in order to produce the required 5 μg of mRNA for hybridization. The samples were hybridized and processed using a Complete GeneChip Instrument System (Scanner, Fluidics Station, Hybridization Oven, and computer workstation).

All the genes were then sorted according to the RP statistic that measures gene differential expression between replicated groups of samples [Breitling et al., 2004], with statistical confidence in form of false discovery rate (FDR) attached to each gene. FDR values were calculated by 100 random permutations of gene ranks on each of the chips. RP method requires that variance of normalized data does not change markedly with the signal mean [Breitling and Herzyk, 2005]. The selected genes were further filtered using the raw data quality control measures, namely the spot confidence (SP) and spot quality (SQ). The quality control requirements set by us were $SP > 0.1$ and $SQ = 1$. For down-regulations, a tight 2.5% FDR was used to select "changed" data, whilst for up-regulation, a generous 50% FDR was used to select changed data. For each gene within the changed datasets, the chromosomal band position was counted and compared to two sets of data from well below the cut-off FDR values (i.e., unchanged data). The data were then plotted for comparison (all Chs and then Chs 3, 11, and 16 specifically).

RESULTS

Scanning electron microscopy (SEM) and AFM was used to image and measure the dimensions of the structures after embossing into PMMA. The EBL pits (with hexagonal (HEX) arrangement) had a final diameter of

120 nm, depth of 100 nm and center–center spacing of 300 nm (Fig. 1A). The columns produced by colloidal lithography (randomly arranged, COL) had a final height of 11 ± 1 nm, diameter of 144 ± 11 nm and center–center spacing of 184 ± 24 nm (Fig. 1A,B).

Image analysis of cell areas showed that fibroblasts reacted to both materials with reduced spreading. In response to COL, the cells were marginally less spread (Fig. 2) and in response to HEX, the cells were significantly less spread, almost to the point of being rounded (Fig. 2).

Chromosome painting of the centromeres of Chs 3, 11, and 16 revealed a general reduction in centromere pair distance (Fig. 3). Specifically, centromeres of cells cultured on COL showed significant decrease for Ch 3, whereas Chs 11 and 16 remained unchanged compared to cells on control. Centromere distance for cells cultured on HEX, however, showed significant decreases for both Chs 3 and 11 compared to control; Ch 16 showed a non-significant decrease.

Microarray results comparing band positions of genes strongly affected by the nanotopographies on all Chs, Ch 3, Ch 11, and Ch 16 plotted versus unaffected genes. It is expected that reduction in cell spreading reduces the number of gene up-regulations and increases the number of gene down-regulations. As has been described, a tight cut-off of a 2.5% FDR was applied from the RP data in order to plot the band positions for the abundant down-regulations and a generous cut-off of 50% FDR was applied for the low number of up-regulations. At 2.5% FDR for fibroblasts cultured on the COL nanotopography this resulted in 11 up-regulations and 190 down-regulations, for fibroblasts

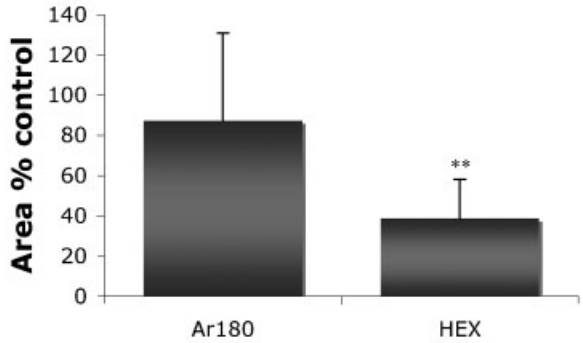

Fig. 2. Cell spreading on the test nanotopographies (hexagonal nanopits (HEX) and nanocolumns (COL)) compared to control. N = 50–60, $^{**}P < 0.01$.

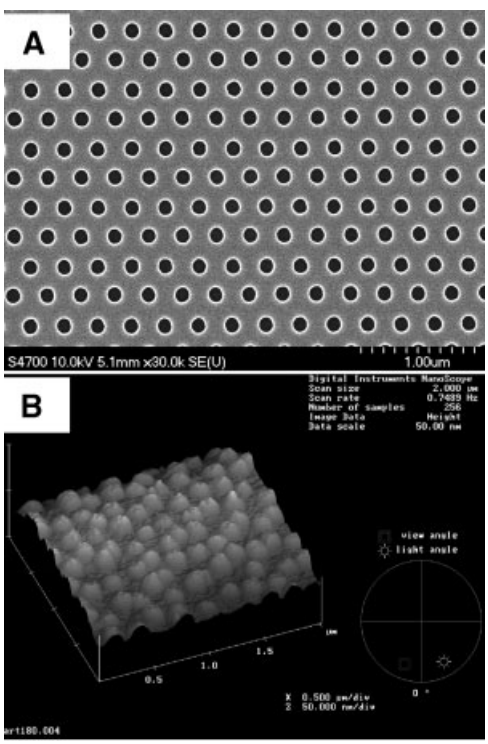

Fig. 1. Nanotopographical surfaces. **A**: SEM images of hexagonal nanopits (HEX). **B**: AFM image of nanocolumns (COL).

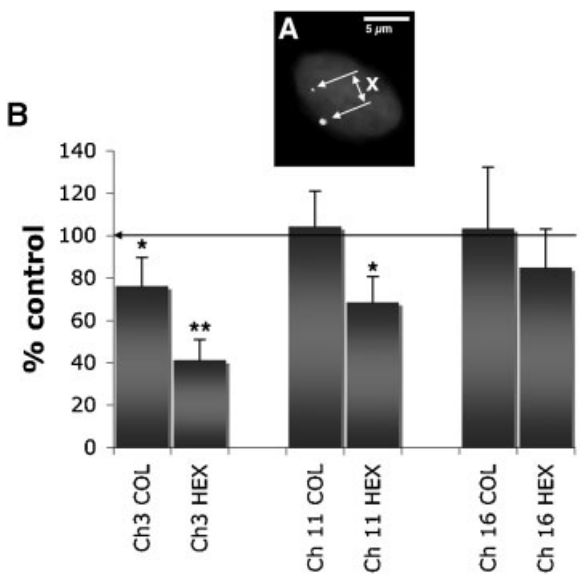

Fig. 3. Measurements of centromere distance. **A**: Image of nucleus with stained centromeres, x represents the distance measured to derive statistics. **B**: Graph showing changes in centromere distances compared to control for cells cultured on the test nanotopographies (hexagonal nanopits (HEX) and nanocolumns (COL)). Centromeres for chromosomes 3, 11, and 16 were labeled. N = 25, $^{*}P < 0.05$, $^{**}P < 0.01$.

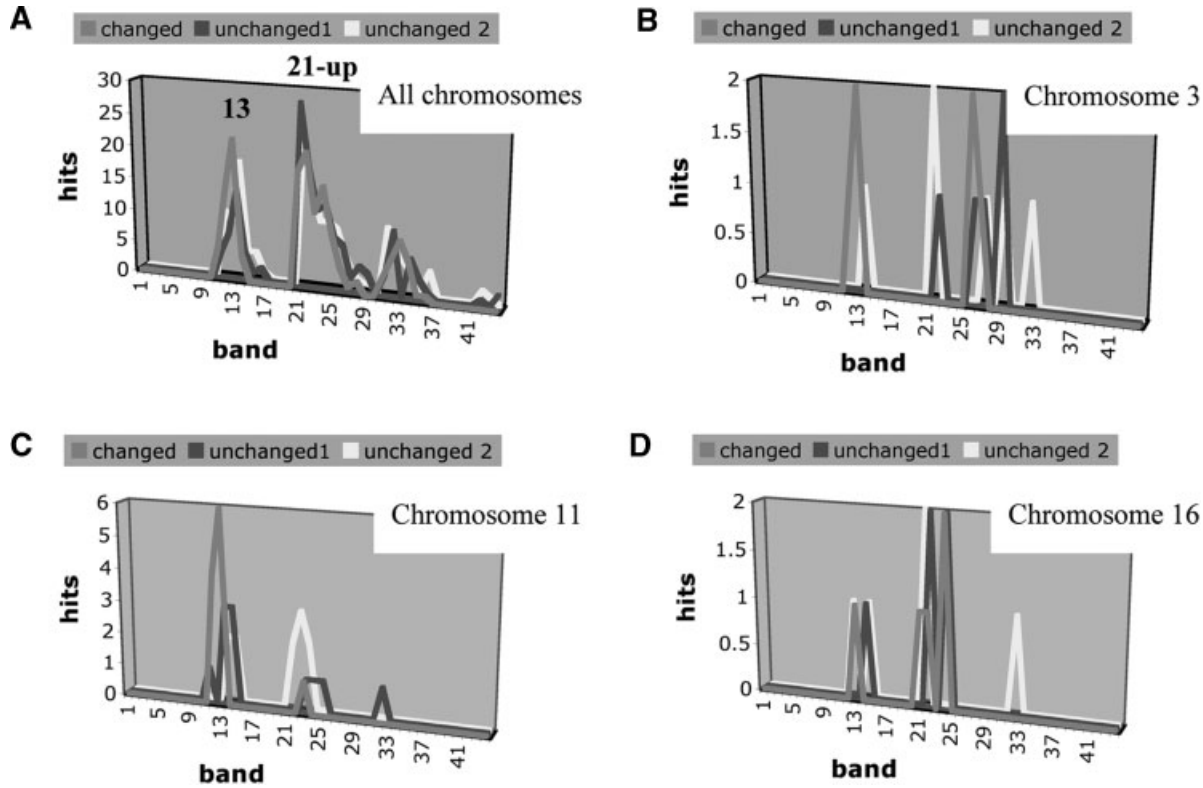

Fig. 4. Plot of band positions on the chromosomal q-arms for down-regulations observed in cells on nanocolumns (COL) (changed) compared band positions of unchanged datasets of similar size (unchanged 1 and 2). Two broad ''peaks'' of genes were observed, one at band 13 and one at band 21-upwards. Note that for all the somatic chromosomes and chromosomes 3 and 11, the changes tend to be within the band 13 grouping compared to the unchanged data profiles. Chromosome 16 shows no change.

on HEX this resulted in 7 up-regulations and 320 down-regulations. Thus, these results fit with previous low-adhesion array profiles [Dalby et al., 2005] where down-regulation is predominant.

The band position profiles for all data on both materials show a loosely biomodal distribution along the Chs, with a peak at around band 13 and then a broader peak around band 21-upwards (Figs. 4–7).

When considering the down-regulations, for cells on COL (all Chs and Chs 3, 11, and 16), there is a general trend of increased down-regulation (changed gene profile compared to those of the unchanged genes) within the first, band 13, grouping. This is most notable for Chs 3 (Fig. 4B) and 11 (Fig. 4C). For cells cultured on HEX, however, the trend is largely reversed. This is apparent in the plots for all Chs and Chs 3 and 11 (Fig. 5A–C). Here, it was seen that there was an increase in down-regulations in the band 21-upwards grouping. The plot for Ch 16, however, showed increased down-regulation in the band 13 grouping (for changed profile compared to unchanged) (Fig. 5D).

When considering the up-regulations, cells on both COL and HEX showed a shifted trend toward up-regulation of genes in the 21-upwards band in most cases (Figs. 6 and 7) (no change in profile was observed for COL on Ch 16 (Fig. 6D)) or for HEX on Ch 11 (Fig. 7C).

DISCUSSION

The results firstly show that nanotopography can be used to reduce cell spreading to different extents. COL produced a slight reduction in cell area and HEX produced a large reduction in cell area. Such effects have been seen with other cell types on similar materials [Gallagher et al., 2002; Dalby et al., 2004].

As cell area is reduced due to nanotopography, so is cytoskeletal organization. It has recently been shown that this reduction in cytoskeletal organization confers a relaxation of nuclear size and lamin organization, that is

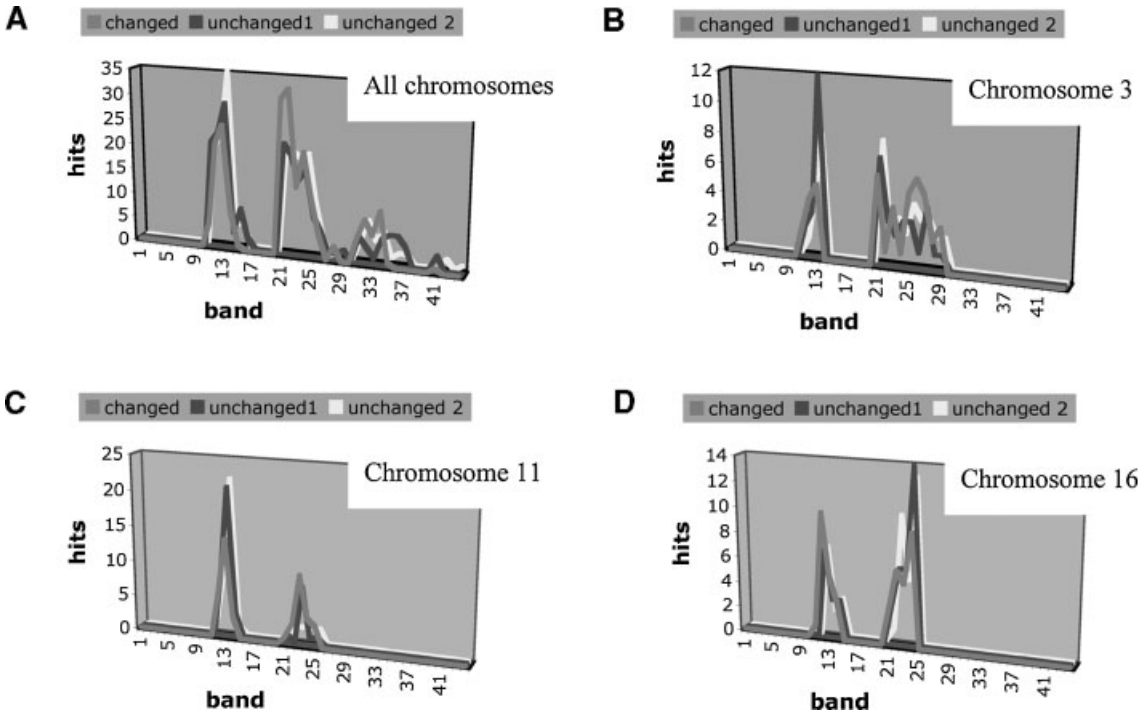

Fig. 5. Plot of band positions on the chromosomal q-arms for down-regulations observed in cells on nanopits (HEX) (changed) compared band positions of unchanged data sets of similar size (unchanged 1 and 2). Two broad ''peaks'' of genes were observed, one at band 13 and one at band 21-upwards. Note that for all the somatic chromosomes and chromosomes 3 and 11, the changes tend to be within the band 21-upwards grouping compared to the unchanged data profiles. Chromosome 16 shows the opposite pattern.

the nuclei become smaller than those of well-spread cells and the lamin network becomes more dense [Dahl et al., 2004; Dalby et al., 2007]. It has also been shown previously that large reductions in cell spreading, such as seen with cells on HEX, lead to changes in relative centromere positioning [Dalby et al., 2007]. This report, however, demonstrates that this effect is more pronounced in the larger somatic Chs with Ch 3 experiencing the largest effects (significant on both COL and HEX), then Ch 11 (significant on HEX only) and finally Ch 16 (no significance). These observations fit with theories of relative interphase organization [Heslop-Harrison, 1992], Ch territories [Cremer and Cremer, 2001] and mechanical principles that the longer elements will experience the greater forces.

The plotting of gene positioning showed a bimodal distribution along the Chs with a first peak around band position 13 and a second, broader, peak around band position 21-upwards. Both low-adhesion topographies lead to a large number of down-regulations, with HEX, the least adhesive, inducing the most down-regulations; this is as expected. However, it seems that the changes are taking place in different band groupings. The COL topography resulted in a larger number of down-regulations in the band 13 grouping (toward the centromere), whilst HEX is resulted in a larger number of down-regulations in the band 21-upwards grouping (toward the telomere). Also apparent from the results is that the larger Chs are, again, the most effected, with little shift observed on Ch 16. For both low-adhesion nanotopographies, the limited numbers of up-regulations observed were noted toward the telomeric positions.

For low-adhesion surfaces where reductions in cell spreading were observed, as the cytoskeleton becomes less organized and the nucleoskeleton more dense, it is possible that this will confer relaxation of mechanical forces to the Chs through interaction of the interphase telomeres with the lamins. This report speculates that a reduction in spreading may have two modes of action depending on the extent of tension release. If tension is released a small amount, it appears that the down-regulations are toward

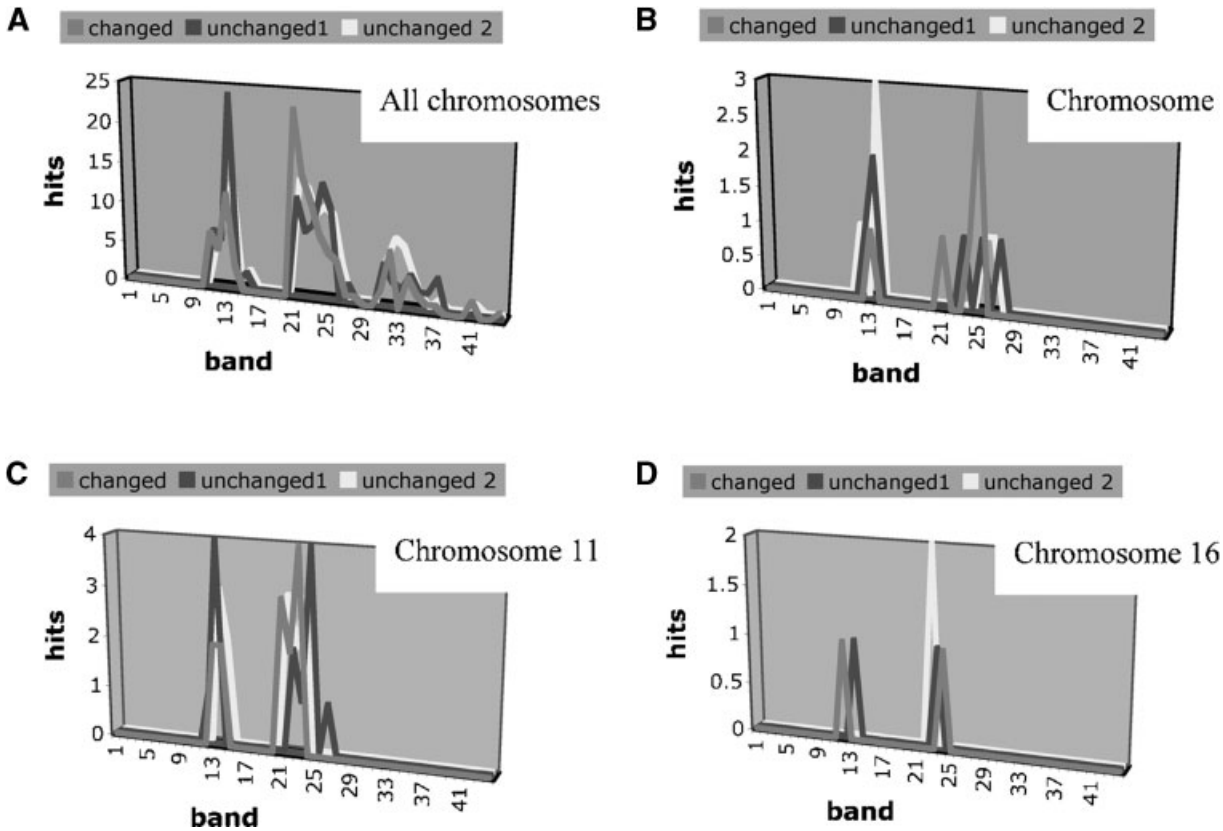

Fig. 6. Plot of band positions on the chromosomal q-arms for up-regulations observed in cells on nanocolumns (COL) (changed) compared band positions of unchanged datasets of similar size (unchanged 1 and 2). Two broad ''peaks'' of genes were observed, one at band 13 and one at band 21-upwards. Note that for all the somatic chromosomes and chromosomes 3 and 11, the changes tend to be within the band 21-upwards grouping compared to the unchanged data profiles. Chromosome 16 showed no change.

the centromeric position. We hypothesize that as tension is released (as the nuclei relaxes), the nuclei becomes more dense and that as the centromeres are more central in the territories than the lamin-associated telomeres, most effect will be experienced here. However, when cell spreading is greatly reduced and the cells retain a more rounded morphology, that is adhesion formation and cytoskeletal organization is at a minimum, the results suggest that the nuclei in its most relaxed morphology is causing down-regulations at the telomeric, peripheral territorial position.

For all up-regulations on these materials, effects were noted at the more telomeric positions. It may be that as the nucleus becomes smaller and the chromosomes more densely packed within the nucleus, diffusion of transcription factors and DNA-dependant enzymes (e.g., polymerases) is firstly reduced toward the center of the chromosome and than as the nuclei relaxes further, diffusion, and thus transcription, is reduced at the telomeres. It is indicated by our results that in all cases of reduced tension, up-regulations will have increased probability at the telomeric regions of the territories.

There have been observations that genes tend to be located at the edge of Ch territories in interphase cells [Mahy et al., 2002; Scheuermann et al., 2004]. This again suggests that the larger the Ch territory (due to size of Ch), the more force will be experienced at the extremes, that is by the genes.

A report by Sun [Sun et al., 2000] suggested that in G1 nuclei, the telomeres of larger Chs are located closer to the nuclear peripheries than those of the small Chs, which ties in well with the results presented here. This could suggest that cells are "pre-wired" for the genome to be mechanosensitive.

In addition, research on application of force to DNA has shown interesting effects with DNA-dependant enzymes [Bryant et al., 2003;

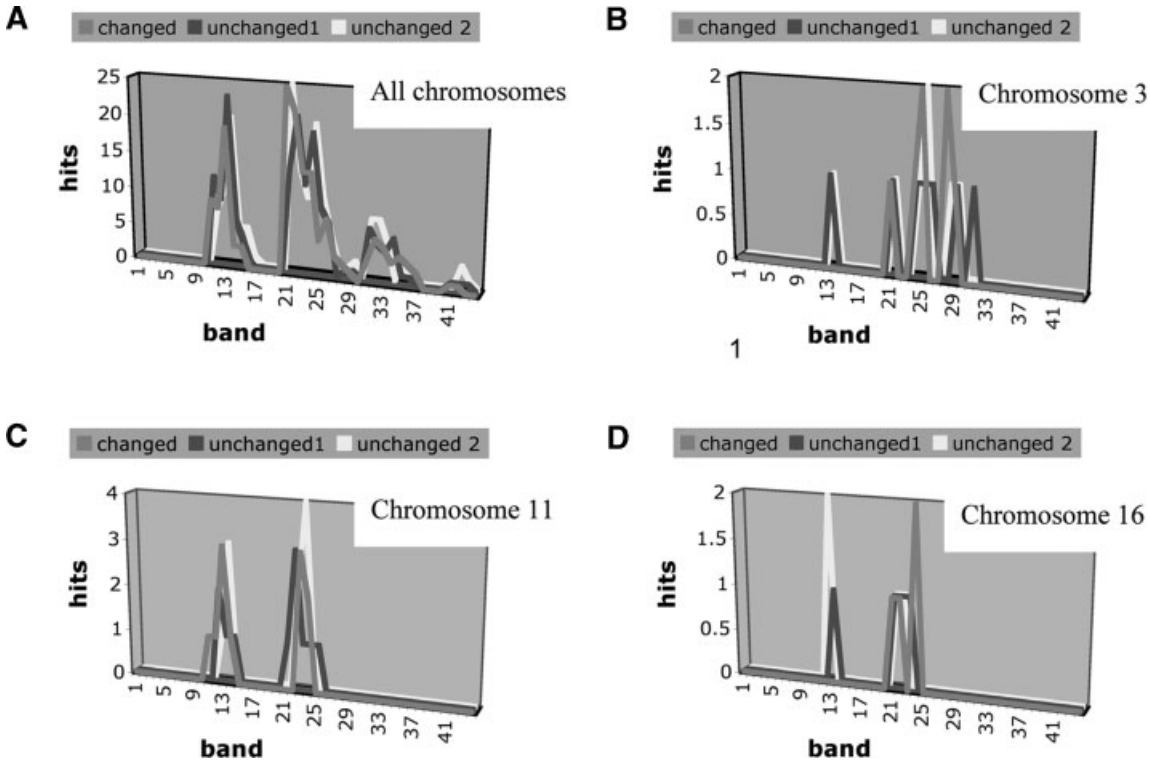

Fig. 7. Plot of band positions on the chromosomal q-arms for up-regulations observed in cells on nanopits (HEX) (changed) compared band positions of unchanged datasets of similar size (unchanged 1 and 2). Two broad ''peaks'' of genes were observed, one at band 13 and one at band 21-upwards. Note that for all the somatic chromosomes and chromosomes 3 and 11, the changes tend to be within the band 21-upwards grouping compared to the unchanged data profiles. Chromosome 11 showed no change.

Bustamante et al., 2003]. RNA polymerase, for example is a powerful motor, generating forces in excess of cytoskeletal motors that drive transport processes within the cell. External loads can, however, affect the tendency of the nuclear enzymes to pause or arrest during transcription. The application of force in an "aiding-direction" reduces pausing. However, unfavorable force can greatly reduce transcription. Thus changes in tension to the nucleus could not only effect diffusion, but also the ability of the enzymes to transcribe efficiently.

This report, along with others, provides evidence for relative Ch positioning being critical to genomic control. They could also relate to comments by Getzenberg [1994] that tissue specific gene expression is intriguing as regulation by single transcription factors cannot be explained simply by DNA sequence, that is the same transcription factor interacting with DNA of different cell types results in different gene expressions despite the similar genome in all cells. Getzenberg then suggests the three-dimensional organization of the genome, structural components of the nucleus and nuclear matrix in different tissues may alter specific gene regulation and could have implications for embryology and development.

We obviously do not discount the indirect mechanotransductive pathways, which are bound to play critical roles in gene regulation, and it is clearly well established that soluble stimuli and changes in surface chemistry can cause changes in cell activity and differentiation of stem cells. However, it is also becoming clear that both the modulus of the matrix [Engler et al., 2006] and the shape of the cells [McBeath et al., 2004] confer changes in differentiation potential for stem cells and that changes in substrate can cause changes in the modulus of the actual cells (via changes in cytoskeleton). For example, it has been reported that mesenchymal stem cells change modulus from 200 to 300,000 Pa depending upon culture material [Simon et al., 2003]. It is likely that morphological changes inferred by topography will give rise to similar changes in modulus and hence be largely responsible for the effects

observed here. We have previously reported that topography can alter mesenchymal stem cell differentiation [Dalby et al., 2006].

We conclude by theorizing that with changing morphologies, tension applied to the nucleus could be critical in determining the probability of gene transcription. Whilst highly speculative, perhaps it is possible to consider release of tension causing the nuclei to act as a collapsing net with most of the collapse felt in an increasingly entangled centromeric position.

ACKNOWLEDGMENTS

MJD is a BBSRC David Phillips Fellow and this research was funded though his fellowship. NG is a Royal Society of Edinburgh Research Fellow. The authors especially thank Dr. Mathis Riehle for guidance and use of his fluorescence microscope. We also thank Dr. Giorgia Riboldi-Turnicliffe, Julie Galbraith, and Jing Wang from the Sir Henry Welcome Functional Genomic Facility.

REFERENCES

Bloom S, Lockard VG, Bloom M. 1996. Intermediate filament-mediated stretch-induced changes in chromatin: A hypothesis for growth initiation in cardiac myocytes. J Mol Cell Cardiol 28:2123–2127.

Breitling R, Herzyk P. 2005. Rank-based methods as a non-parametric alternative of the t-statistic for the analysis of biological microarray data. J Bioinform Comput Biol 3: 1171–1190.

Breitling R, Armengaud P, Amtmann A, Herzyk P. 2004. Rank products: A simple, yet powerful, new method to detect differentially regulated genes in replicated microarray experiments. FEBS Lett 573:83–92.

Bryant Z, Stone MD, Gore J, Smith SB, Cozzarelli NR, Bustamante C. 2003. Structural transitions and elasticity from torque measurements on DNA. Nature 424: 338–341.

Burridge K, Chrzanowska-Wodnicka M. 1996. Focal adhesions, contractility, and signaling. Annu Rev Cell Dev Biol 12:463–518.

Bustamante C, Bryant Z, Smith SB. 2003. Ten years of tension: Single-molecule DNA mechanics. Nature 421: 423–427.

Charras GT, Horton MA. 2002. Single cell mechanotransduction and its modulation analyzed by atomic force microscope indentation. Biophys J 82:2970–2981.

Clark P, Connolly P, Curtis AS, Dow JA, Wilkinson CD. 1991. Cell guidance by ultrafine topography in vitro. J Cell Sci 99(Pt 1):73–77.

Cremer T, Cremer C. 2001. Chromosome territories, nuclear architecture and gene regulation in mammalian cells. Nat Rev Genet 2:292–301.

Dahl KN, Kahn SM, Wilson KL, Discher DE. 2004. The nuclear envelope lamina network has elasticity and a compressibility limit suggestive of a molecular shock absorber. J Cell Sci 117:4779–4786.

Dalby MJ. 2005. Topographically induced direct cell mechanotransduction. Med Eng Phys 27:730–742.

Dalby MJ, Riehle MO, Sutherland DS, Agheli H, Curtis AS. 2004. Changes in fibroblast morphology in response to nano-columns produced by colloidal lithography. Biomaterials 25:5415–5422.

Dalby MJ, Riehle MO, Sutherland DS, Agheli H, Curtis AS. 2005. Morphological and microarray analysis of human fibroblasts cultured on nanocolumns produced by colloidal lithography. Eur Cell Mater 9:1–8; discussion 8.

Dalby MJ, McCloy D, Robertson M, Wilkinson CDW, Oreffo ROC. 2006. Osteoprogenitor response to defined topographies with nanoscale depths. Biomaterials 27:1306–1315.

Dalby MJ, Biggs MJP, Gadegaard N, Kalna G, Wilkinson CDW, Curtis ASG. 2007. Nanotopographical stimulation of mechanotransduction and changes in interphase centromere positioning. J Cell Biochem 100:326–338.

Denis FA, Hanarp P, Sutherland DS, Dufrene YF. 2002. Fabrication of nanostructured polymer surfaces using colloidal lithography and spin coating. Nanoletters 2: 1419–1425.

Eastwood M, McGrouther DA, Brown RA. 1998. Fibroblast responses to mechanical forces. Proc Inst Mech Eng [H] 212:85–92.

Engler AJ, Sen S, Sweeney HL, Discher DE. 2006. Matrix elasticity directs stem cell lineage specification. Cell 126: 677–689.

Fey EG, Wan KM, Penman S. 1984. Epithelial cytoskeletal framework and nuclear matrix-intermediate filament scaffold: Three-dimensional organization and protein composition. J Cell Biol 98:1973–1984.

Forgacs G. 1995. On the possible role of cytoskeletal filamentous networks in intracellular signaling: An approach based on percolation. J Cell Sci 108(Pt 6): 2131–2143.

Foster HA, Bridger JM. 2005. The genome and the nucleus: A marriage made by evolution. Genome organisation and nuclear architecture. Chromosoma 114:212–229.

Gadegaard N, Thoms S, MacIntyre DS, McGhee K, Gallagher J, Casey B, Wilkinson CDW. 2003. Arrays of nano-dots for cellular engineering. Microelectronic Eng 67–68:162–168.

Gallagher JO, McGhee KF, Wilkinson CDW, Riehle MO. 2002. Interaction of animal cells with ordered nanotopography. IEEE Trans Nanobiosci 1:24–28.

Getzenberg RH. 1994. Nuclear matrix and the regulation of gene expression: Tissue specificity. J Cell Biochem 55: 22–31.

Hanarp P, Sutheraland DS, Gold J, Kasemo B. 2003. Control of nanoparticle film structure for colloidal lithography. Colloids Surf A 214:23–36.

Heslop-Harrison JS. 1992. Nuclear architecture in plants. Curr Opin Genet Dev 2:913–917.

Heslop-Harrison JS, Leitch AR, Schwarzacher T. 1993. The Physical organisation of interphase nuclei. In: Heslop-Harrison JS, Flavell RB, editors. The Chromosome. Oxford: Bios. p 221–232.

Hoskins GC. 1965. Electron microscopic observations of human chromosomes isolated by micrurgy. Nature 207: 1215–1216.

Ingber DE. 1993. Cellular tensegrity: Defining new rules of biological design that govern the cytoskeleton. J Cell Sci 104(Pt 3):613–627.

Ingber DE. 2003a. Tensegrity I. Cell structure and hierarchical systems biology. J Cell Sci 116:1157–1173.

Ingber DE. 2003b. Tensegrity II. How structural networks influence cellular information processing networks. J Cell Sci 116:1397–1408.

Katsumi A, Orr AW, Tzima E, Schwartz MA. 2004. Integrins in mechanotransduction. J Biol Chem 279: 12001–12004.

Mahy NL, Perry PE, Gilchrist S, Baldock RA, Bickmore WA. 2002. Spatial organization of active and inactive genes and noncoding DNA within chromosome territories. J Cell Biol 157:579–589.

Maniotis AJ, Bojanowski K, Ingber DE. 1997a Mechanical continuity and reversible chromosome disassembly within intact genomes removed from living cells. J Cell Biochem 65:114–130.

Maniotis AJ, Chen CS, Ingber DE. 1997b. Demonstration of mechanical connections between integrins, cytoskeletal filaments, and nucleoplasm that stabilize nuclear structure. Proc Natl Acad Sci USA 94:849–854.

Martines E, Seunarine K, Morgan H, Gadegaard N, Wilkinson CDW, Riehle MO. 2005. Superhydrophobicity and superhydrophilicity of regular nanopatterns. Nanoletters 5:2097–2103.

McBeath R, Pirone DM, Nelson CM, Bhadriraju K, Chen CS. 2004. Cell shape, cytoskeletal tension, and RhoA regulate stem cell lineage commitment. Dev Cell 6:483–495.

Molenaar C, Wiesmeijer K, Verwoerd NP, Khazen S, Eils R, Tanke HJ, Dirks RW. 2003. Visualizing telomere dynamics in living mammalian cells using PNA probes. EMBO J 22:6631–6641.

Scheuermann MO, Tajbakhsh J, Kurz A, Saracoglu K, Eils R, Lichter P. 2004. Topology of genes and nontranscribed sequences in human interphase nuclei. Exp Cell Res 301:266–279.

Simon A, Cohen-Bouhacina T, Porte MC, Aime JP, Amedee J, Bareille R, Baquey C. 2003. Characterization of dynamic cellular adhesion of osteoblasts using atomic force microscopy. Cytometry A 54:36–47.

Sun HB, Shen J, Yokota H. 2000. Size-dependent positioning of human chromosomes in interphase nuclei. Biophys J 79:184–190.

Wang N, Suo Z. 2005. Long-distance propagation of forces in a cell. Biochem Biophys Res Commun 328:1133–1138.

Whitesides GM. 2003. The 'right' size in nanobiotechnology. Nat Biotechnol 21:1161–1165.